Computers & Geosciences 44 (2012) 184–195

Contents lists available at SciVerse ScienceDirect

Computers & Geosciences

journal homepage: www.elsevier.com/locate/cageo

Implementation of Martian virtual reality environment using very high-resolution stereo topographic data

Jung-Rack Kim [a,*], Shih-Yuan Lin [b], Jeong-Woo Hong [c], Young-Hwi Kim [d], Chin-Kang Park [e]

[a] Department of Geoinformatics, University of Seoul, Seoul, Republic of Korea
[b] Department of Land Economics, National Chengchi University, Taipei, Taiwan
[c] Korea Institute of Science and Technology Information, Daejeon, Republic of Korea
[d] Yonsei University, Seoul, Republic of Korea
[e] Korea Advanced Institute of Science and Technology, Daejoon, Republic of Korea

ARTICLE INFO

Article history:
Received 15 July 2011
Received in revised form
29 September 2011
Accepted 30 September 2011
Available online 21 October 2011

Keywords:
Mars
High resolution DTM
Ortho-image
Virtual reality
Stereo analysis
Geomorphology

ABSTRACT

Topography over terrestrial or other planetary surfaces is an important base data for virtual reality construction. In particular, with inaccessible topography such as the Martian surface, virtual reality provides great value not only for public interaction but also for scientific research. For the latter application, since field surveys are essential for the geological and geomorphological researches, the virtual reality environment created based on verified topographic products provides an alternative solution for planetary research.

The performance of virtual reality implementation over a planetary surface can be assessed by two major factors: (1) The geodetically controlled base topographic products, such as DTM and ortho-image, and (2) Technological integration of topographic products into virtual reality software and hardware. For the first aspect, the multi-resolution stereo analysis approach has already provided a solid basis so that specific topographic data sets over testing areas were generated by the hierarchical processor. To address the second problem, a parallel processor with multiple screen display combining 3D display software was employed in this research.

As demonstrated in this paper, the constructed Martian virtual environment showed highly detailed features over the Athabasca Valles (one of former potential Mars Exploration Rover landing sites) and Eberswalde crater (one of the main original landing candidates for the NASA's rover mission scheduled to launch in late 2011). The employment of such virtual reality environments is expected to be a powerful simulator after integrating a 3D Martian model, engineering and environment constraints for Martian geological and geomorphic researches including landing site selection and rover navigation.

1. Introduction

High-resolution satellite imagery and 3D topographic products (e.g. digital terrain model (DTM)) constructed from orbital image data have been recognized as important tools for investigating planetary topography. Geological and geomorphological analyses and interpretation can be performed effectively and precisely (Warner et al., 2009, 2010a,b) exploiting such planetary 3D topographic products. Therefore, in order to extract more detailed information, orbital sensors capable of capturing images with advanced spatial resolution should be employed in planetary exploration missions. The High Resolution Imaging Science Experiment (HiRISE) and Context Camera (CTX) onboard the Mars Reconnaissance Orbiter (MRO) are successful examples. Due to the advantage of improved orbital image quality, the construction of 3D topographic products with higher spatial resolution has also become achievable (Kirk et al., 2003, 2008; Kim and Muller, 2009).

The usage of high resolution topographic products is not only beneficial for studying 3D structures and formation of geomorphological features, but it is also required for in-situ exploration of the Martian surface, including the Martian rover's landing site selection and traverse navigation. For the application of landing site selection, the topographic products are critical for investigating the scientific research interest and assessing engineering constraints over candidate landing sites (Kirk et al., 2008). Moreover, the rover's traversing and maneuvering were achieved in the Martian environment simulation whose construction was based on the imagery acquired by the panoramic camera installed on the rover. Due to the viewing angle of the camera and the time for data transferring and processing, the capability to pre-investigate the exploration areas was limited. This issue can be addressed if

* Corresponding author. Tel.: +82 7082533008; fax: +82 222460186.
E-mail address: kjrr001@gmail.com (J.-R. Kim).

0098-3004/$ - see front matter © 2011 Elsevier Ltd. All rights reserved.
doi:10.1016/j.cageo.2011.09.018

the navigation simulator is enhanced with precisely controlled topographic products from orbital stereo imagery.

As stated above, the key factor for successful geological analyses and in-situ exploration is Martian topographic data with high spatial resolution and photogrammetric quality. In order to fully utilize various orbital images, the generalized algorithms of image processing and photogrammetric Mars DTM extraction have been developed and implemented by Kim and Muller (2009), in which a non-rigorous sensor model and hierarchical geodetic control were employed. Due to the successful "from coarse to fine" control strategy performed during processing, stable horizontal and vertical photogrammetric accuracy of resultant Mars DTM was achieved compared with Mars Obiter Laser Altimeter (MOLA) DTM. Recently, the algorithms developed by Kim and Muller (2009) were further updated by employing an advanced image matcher in matching iterative window selection and improved sensor model strategy as described in this paper. The algorithms have been successfully applied to CTX and HiRISE stereo image data to produce DTMs and ortho-rectified images. More details are given in the following section.

A virtual reality (VR) system is powerful tool allowing scientists and public users to explore in a simulated environment. In order to accomplish a simulation with high level of details, the quality of the utilized topographic products plays an important role. Since the updated photogrammetric processing line is capable of producing a co-aligned geodetically topography, it is further proposed to establish a VR environment employing the topographic products created in this study. The topographic data were incorporated into a VR system provided by the Korea Institute of Science and Technology Information (KISTI) and demonstrated over the potential Mars rover landing sites.

2. Martian topographic data extraction and verification

Martian imagery and topographic data produced by stereo processing comprise an essential basis for the establishment of virtual reality. The first accurate systematic topographic measurements were the Mars Orbiter Laser Altimeter (MOLA) experimenters of Mars Global Surveyor (MGS) launched on the 7th of November 1996 (Smith et al., 2001). Given its high accuracy (Neumann et al., 2001) achieved by the cross-over track analysis and global coverage, the MOLA data is considered as the most consistent Mars DTM and treated as a "base topography" (Heipke et al., 2007; Kim and Muller, 2008). However, the best resolution of MOLA DTM over area between $\pm 88^{\circ}$ latitude (463 m per pixel; Jaumann et al., 2007) is insufficient for the purposes of this study.

The possibility of Martian stereo topography construction was initially tested using stereo-pairs acquired by the Viking Orbiter and Mars Orbiter Camera Narrow Angle (MOC-NA) for the landing site survey of the Mars Exploration Rover (MER) by Kirk et al. (2003). Then the HRSC instrument onboard ESA's Mars Express, capable of capturing images of 12.5 m spatial resolution, addressed the limitation of available resolution and stereo image coverage over the Martian surface (Albertz et al., 2005; Scholten et al., 2005). It was further reported that the construction of Martian DTMs with grid spacing of 30–75 m with HRSC stereo imagery was achievable (Gwinner et al., 2007; Heipke et al., 2007; Kim and Muller, 2009). It is worth noting that the photogrammetric processing strategy using gridded MOLA DTM for HRSC guarantees very stably controlled topographic products (Spiegel, 2007). Moreover, compared with the MOLA DTM, the resolution of the HRSC DTM is significantly improved and highly valuable as the photogrammetric reference surface for the processing of other imagery.

In late 2006, the successful deployment of the NASA MRO with the CTX and HiRISE instruments began to provide repeat-pass stereo image pairs. The spatial resolution of acquired imagery was further upgraded to 6 m and 25 cm, thereby providing an opportunity to produce very high resolution DTMs (Malin et al., 2007; McEwen et al., 2007). Through the developed algorithms, Kim and Muller (2009) produced CTX DTMs with grid spacing of 12–20 m. For stereo HiRISE data processing, Kirk et al. (2008) and Kim and Muller (2009) demonstrated that the resolution of processed HiRISE DTM was up to one meter or even sub-meter level.

The topographic products introduced above provide great value to scientists who need DTMs for diverse Mars explorations. These data sets are obtained from different sensors and have various characteristics. Therefore there will be additional benefits, e.g. simultaneous observation of multiple topographic data, if multiple topographic products can be correctly co-registered. To achieve this, a robust geodetic control method was implemented. Since the MOLA DTM provides an accurate global topographic data set (Neumann et al., 2001), it is used as the reference surface. The other DTMs are then aligned to fit MOLA. However, considering the magnitude difference in DTM resolution between MOLA and other DTMs, a hierarchical approach applying surface matching was proposed. The HRSC DTM was first employed as an intermediate data set and matched to the MOLA DTM. The matched HRSC DTM was subsequently adopted as the reference surface in a surface matching with CTX DTM. As the HRSC DTM could provide more terrain features than MOLA and it had been co-registered with MOLA, it was suitable to replace MOLA in the case of fusion with a CTX DTM. In the same manner, the co-registered CTX DTM was employed as the reference terrain model in a surface matching with HiRISE DTM. As a result, a co-registration of all four DTMs was achieved. This is the key idea of Kim and Muller's (2009) approach, and the technical details of geodetic matching between different topographic data sets were provided in Lin et al. (2010).

2.1. Topographic data processing

Combining the accurate stereo matching system together with the robust geodetic control, the resultant topographic products, especially CTX and HiRISE DTMs and ortho-images, are proposed as the base data for VR establishment. The detailed processing schemes for HRSC, CTX and HiRISE data are described below.

2.1.1. HRSC processing

The extraction of HRSC DTM in this study was based on the DLR-VICAR (Video Image Communication and Retrieval) combined with an indigenous two-stage stereo image matcher. The DLR-VICAR software was developed by the German Aerospace Centre (DLR) and was employed for the photogrammetric processing of HRSC data (Scholten et al., 2005; Albertz et al., 2005). The two-stage image matcher replacing the original matcher of DLR VICAR in this research consisted of a front end image matcher based on the algorithm developed by Zitnick and Kanade (2000) together with the quasi epipolarity of the HRSC Level-2 data and the subsequent refinement scheme by the Adaptive Least Squares Correlation (ALSC; Gruen, 1985; Day and Muller, 1989), which update the sub-pixel matching accuracy of high density seed points derived from the front end matcher. The 3D coordinates of the matched points were then computed by space intersection component of DLR-VICAR photogrammetric processing routine.

The quality of image matching was largely influenced by the quality of the ortho-images imported into the image matching step and the applied matching parameters, such as matching window size. Therefore to improve the matching accuracy, an iterative strategy of image matching with a set of matching parameters in hierarchical levels was carried out. This scheme was based on the idea that the base DTM can be iteratively updated and the search space and the window for matching cost calculation can be smaller at each iteration. Therefore, the topographic details were preserved, while matching blunders could be minimized.

2.1.2. CTX processing

For CTX processing, the full non-rigorous sensor model was introduced. This approach has been used for the commercial satellite imagery for decades and now possesses accuracy comparable to that of the conventional physical sensor model, as demonstrated in many photogrammetric applications (Dowman and Dolloff, 2000; Tao and Hu, 2002; Fraser et al., 2006). Regarding the Martian data, Kim et al. (2007) have examined the availability of a non-rigorous model for the Martian imagery and showed that a 'few pixels' level positioning error could be achieved.

For the task of geodetic control, as the resolution of HRSC data is higher than MOLA products, and considering that the HRSC pixel has an inherent planimetric accuracy of 25–40 m and a 3D space intersection of up to 6–8 m vertical co-registration with MOLA (Spiegel, 2007), Kim and Muller (2009) reported that the HRSC intersection points and ortho imagery were capable of being employed for the geodetic control of CTX and HiRISE. Therefore the photogrammetric products from HRSC processing and co-registration were used for the geodetic control of CTX stereo images.

The image matching of the CTX image processing is basically identical to the HRSC matching scheme but employs the "bigger matching window first" stereo matching strategy. When performing image matching for CTX, the matching results derived from the biggest matching window were employed as the base data. They were then compared against the matching outputs obtained from the smaller matching window size in the next iteration. Then the base data was replaced by the matching point produced by a smaller window once the difference was within some critical value decided by the limit of the local natural slope (45°), which is the criterion of natural geomorphology and matching error.

2.1.3. HiRISE processing

The main difficulty of HiRISE stereo processing occurred at the data pre-processing stage, resulting from the special sensor structure. At this stage it was necessary to combine 20 red CCD channels into a single frame HiRISE image (i.e. a Level-1 HiRISE image). The other issue was the removal of HiRISE camera distortion originating from high frequency pointing oscillation, the so-called "jitter effect"; detector offsets also occurred between overlapping CCD detectors (Kirk et al., 2008). To deal with the image deformation, a number of functions in the Integrated Software for Imagers and Spectrometers (ISIS) software (Anderson et al., 2004; USGS, 2009), such as "spacefit", "cam2cam", "noproj", etc., were performed to create an undistorted Level-1 HiRISE image based on an idealized camera model (Kirk et al., 2008). In addition, a complementary HiRISE image projected over the Martian ellipsoid was produced (i.e., a Level-2 HiRISE image). The Level-2 HiRISE images were subsequently used for control point setup and stereo image matching. An add-on program was also developed for the coordinate transformation and the reverse transformation between the Level-1 and Level-2 HiRISE images.

With these procedures, the HiRISE photogrammetric processing employed the unified non-rigorous sensor modeling method. For the geodetic control of the HiRISE non-sensor model, the DTM and ortho-image products from the CTX processing line were employed as reference data.

2.2. Test sites

Eberswalde crater is an impact crater located at 24.2°S latitude and 326.5°E longitude in the southern highlands of Mars, near north of Holden crater. The crater is a drainage basin of a ~90 km-long fluvial network where the channel system debouches into the crater, and a ~150 m-thick fan of material is distributed across 10 km by 25 km of the crater floor (Malin and Edgett, 2003), comprising lobes. The deposit within crater is supposed to be a river delta formed within a standing crater lake (Malin and Edgett, 2003; Moore et al., 2003) or an alluvial fan (Jerolmack et al., 2004). In detail, Malin and Edgett (2003) interpreted it as an exhumed and inverted remnant of fluvial distributary network in late Noachian age. Moore et al. (2003) estimated persistent 700 m^3/s water based on the channel width and meander wavelength. If the origin of water flow was the quasi-periodic climate involving typical terrestrial-style precipitation, it required 10^3–10^6 years to form the whole deposit according to their assumption. A quantitative analysis of the exposed stratigraphy by Lewis and Aharonson (2006) made the conclusion that the delta likely formed not in a stable long-lived lake but over the course of a small number of shorter lacustrine episodes, which were not sustained at equilibrium conditions. Therefore, it was proposed as one of the two finalists for the NASA's rover mission scheduled to land in August 2012 due to its clear fluvial origin. It is noted that the quality of the DTM plays a key role for correctly determining fan deposits and morphologic parameters of the channel network system. Compared with the MOC-NA stereo pairs employed in Moore et al. (2003) and Lewis and Aharonson (2006), the DTMs reconstructed from high-resolution HiRISE and CTX stereo imagery definitely improve the correctness and efficiency for geological and morphologic analyses.

Athabasca Valles (center latitude and longitude of this area is 8°N and 156°E, respectively) is a controversial area due to a complex history of recent fluvial (Burr et al., 2002; Murray et al., 2005) and volcanic (Plescia, 2003; Jaeger et al., 2007) activities. The central Valles were likely formed by catastrophic flood, which was dated into very recent geological activity, probably originated from the groundwater eruption by the thermal activities in Cerberus Fossae (Head et al., 2003). In addition, the teardrop streamlined forms and the longitudinal lineation in the Athabasca Valles were proposed as very supportive evidences for the recent fluvial in the central channel as noted by Burr et al. (2002). On the contrary, Jaeger et al. (2007) argued that polygonal, ridged flow textures and widely populated cone structures (so called ring-mound landforms) observed in detail by HiRISE image were the results of thin low-viscosity fluid lava flow from the Cerberus. Later, Jaeger et al. (2010) proposed a single eruption covering 250,000 km^2 of western Elysium Planitia with an estimated 5000–7500 km^3 of mafic or ultramafic flood lava emplaced turbulently over a period of only a few to several weeks.

Athabaca Valles was also the object of intense scrutiny as surface ageing might be contaminated by the secondary craters from Crater Zunil (McEwen et al., 2005). In addition to these scientific interests, considering the engineering safety of a future rover in the well-eroded and extremely flat geomorphology, Athabasca Valles had been selected as a candidate for the landing place for the Mars Exploration Rover. For all above topics about the geological implication over Athabasca Valles, the multi-resolution DTMs would provide crucial information, such as the detailed 3D model of cones, the finest terrain over the floor of the Valles, and the tear-drop shaped island structures.

2.3. Results and validation

The whole Eberswalde crater, including the origin of fluvial channel, was covered with three HRSC orbital images (h2002_0000, h2013_0000, h2024_0000) with 12.5 m nadir image resolution. The DTM mosaic from these stereo images was constructed with 50 m and 70 m grid spacing at first. The main lobes of fluvial deposit fans are well included with high quality CTX stereo coverage from two stereo pairs (P01_001336_1560, P01_001534_1559 and B02_010474_1558, P01_010553_1558). Topographic products including

18 m grid spacing CTX DTMs and 6 m ortho-images were processed individually with the geodetic control from HRSC DTMs. Subsequently the two stereo DTMs and ortho-images are mosaicked together. It was found that a HiRISE stereo pair (PSP_001336_1560 and PSP_001534_1560) was located in the central part of CTX topographic products. Additionally, another HiRISE pair with ESP_018412_1560 and ESP_016777_1560 was published in the eastern part of the channel (see Fig. 1(a)). These HiRISE pairs were processed into 2.1 m (ESP_018412_1560 and ESP_016777_1560) and 3.7 m (PSP_001336_1560 and PSP_001534_1560) grid spacing, according to the image quality based on the geodetic control of CTX topographic products. The part of PSP_001336_1560 and PSP_001534_1560 stereo coverage was processed into 1 m resolution DTM.

It was understood that high resolution DTMs are essential in investigating the geological origin of Athabasca Valles area as well as forecasting potential risks around the landing zone. The MOLA DTM with 463 m does not show sufficient detail on Athabasca channel geomorphology and streamline island shape, e.g. the boundary and the depth of the channel for such purposes. However, the central part of the channel is covered by a HRSC high-resolution image (in Athabasca, h2099_0099) whose nadir image resolution is 12.5 m, so the image matching scheme can have this image applied and reconstruct 50 m DTMs. Then a CTX stereo DTM generated from images P01_001540 and P02_001504_1889 can be extracted from geodetic control using HRSC intersection points. At last, HiRISE DTM was constructed using PSP_001540_1890 and PSP_002371_1890 with the geodetic control from CTX DTM and ortho-image. The image coverage over Athabasca test site is shown in Fig. 1(b). A DTM with 2.5 m grid spacing and 40 cm ortho-image was extracted for the whole HiRISE stereo coverage and then a refinement was performed to upgrade the resolution of DTMs to 0.75 m for a sub area.

The processed DTMs and ortho-images over Eberswalde crater and Athabasca Valles are shown in Figs. 2 and 3, respectively. The overlapped products in Eberswalde between CTX and HiRISE stereo pairs are mosaicked together as shown in Fig. 2(b) and (c). It is worthwhile noting that the resultant topographic products are purely made by the algorithm execution without any manual editing. From the visual observation, the performance of developed processing software is clearly demonstrated.

In order to show the potential of the stereo processing line, the HRSC and CTX DTMs are processed to achieve the best possible grid spacing. As a result, very few blunders are shown (as seen in Figs. 2(a), (b) and 3(a), (b)) and the stability of the applied stereo algorithms is proved. For HiRISE DTMs with the best grid spacing up to sub-meter in Athabasca and Eberswalde (see Figs. 2(d) and 3(d)), it is normally unavoidable to include a few artifacts especially in the overlapped parts of each CCDs as shown in parts labeled "A" of Figs. 2(d) and 3(d). This "jitter effect" originated from the instability of camera pointing and amplified in every 20 CCD overlapped portion (refer to Kirk et al., 2008 for the detailed

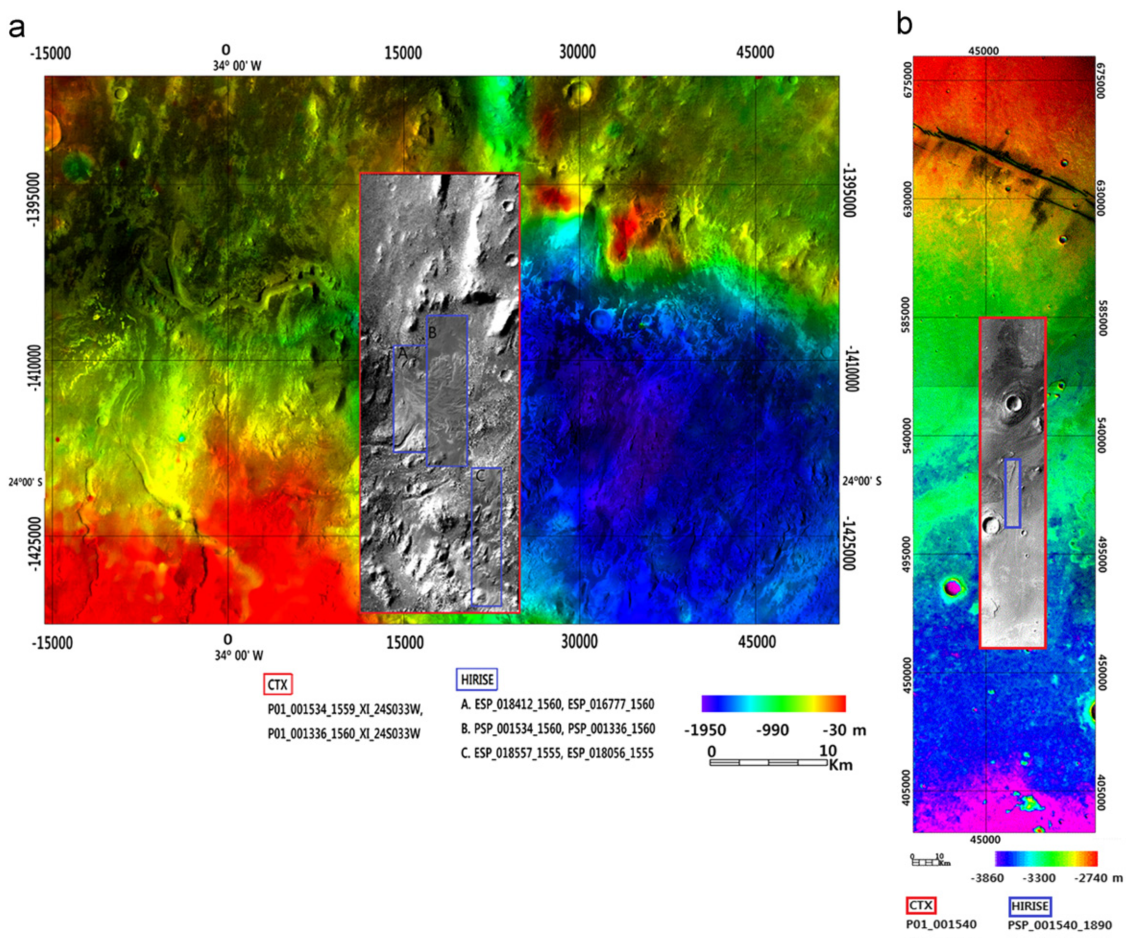

Fig. 1. The coverage of CTX and HiRISE stereo over target areas. The background is colorized by height hill-shaded HRSC DTM. (a) CTX and HiRISE image coverage over Eberswalde crater. (b) CTX and HiRISE image coverage over the Athabasca Valles.

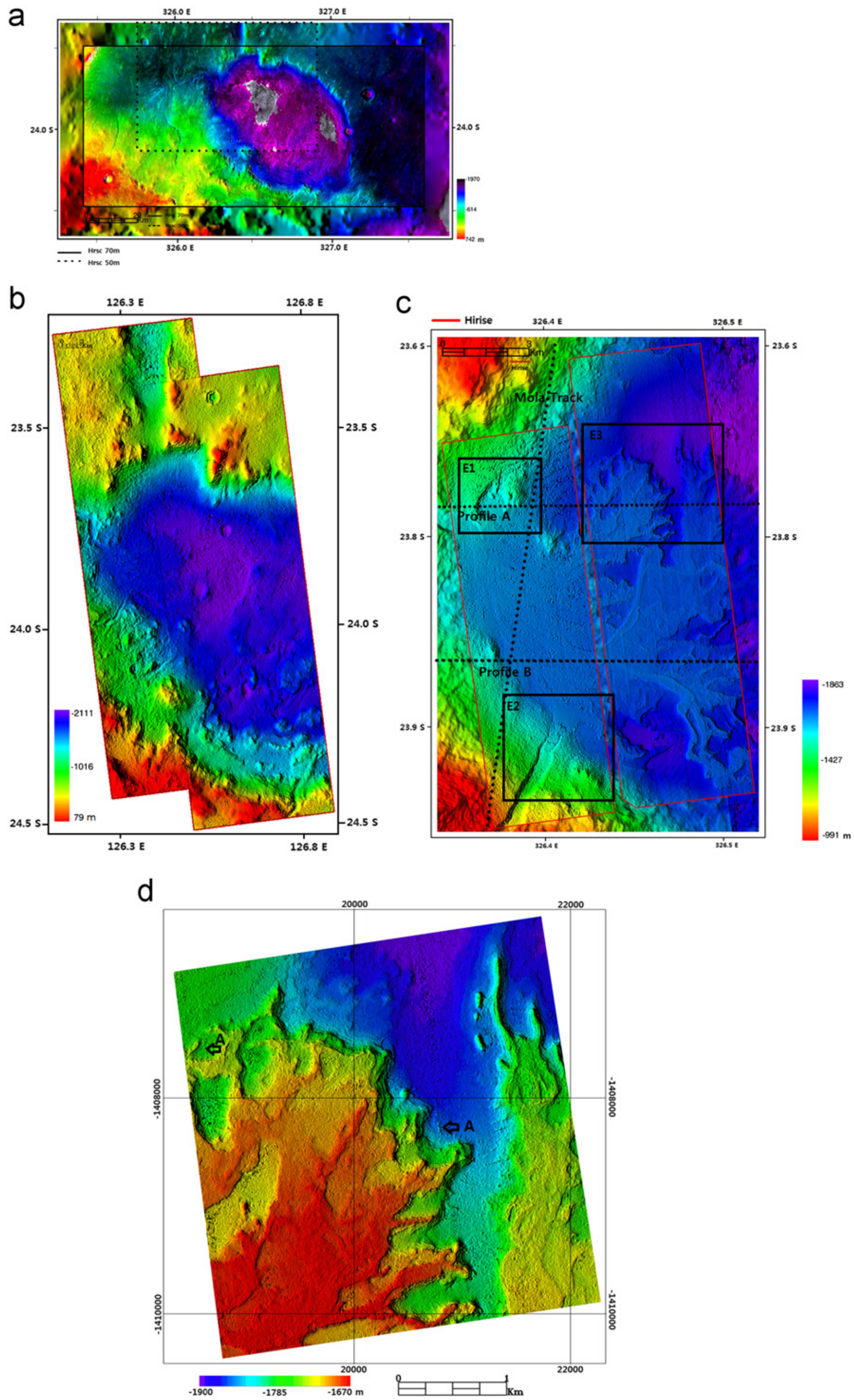

Fig. 2. The CTX and HiRISE topographic products of the Eberswalde crater. (a) 70 m resolution HRSC DTM over Eberswalde Crater (black box) and 50 m resolution refined HRSC DTM (dotted box). (b) 18 m CTX DTM mosaic by two CTX stereo DTMs over Eberswalde. It should be noted there is no huge discontinuity (> 20 m vertically) crossing two CTX Stereo DTMs. (c) Two HiRISE DTMs (left: 3.7 m resolution, right: 2.1 m resolution) mosaic over CTX stereo DTM background. See Fig. 9(a)–(c) for the detailed VR implementations over E1, E2 and E3 subareas. (d) Refined 1 m HiRISE DTM over the part of lobes.

description). Except for these artifacts, it is observed that the HiRISE DTM did not include any distinguished faults as shown in hill-shaded images.

Since the topographic products were created, another critical issue is the determination of vertical and horizontal accuracy of the products. As the cross-over inter-track control using least squared fitting provided the absolute positioning accuracy for each laser altimetry point measurement (Neumann et al., 2001) over the IAU 2000 Martian ellipse, MOLA can be used not only as the base control plane of all photogrammetric Martian products but also as a good standard data set for the stereo DTM assessments. However, in the assessment procedure using MOLA height spots, it should be noted that there is difficulty in comparing a variety of DTMs with different spatial resolutions. Moreover, it is still not clear how the local height variation within MOLA footprints affect the measured beam centroid, although this issue was initially explored by Gardner (1992) and especially by Neumann et al. (2003) and Kim and Muller (2008) for Martian case.

Considering the constraints described above, the topographic products with a unified intermediate resolution, hereby 18 m, were

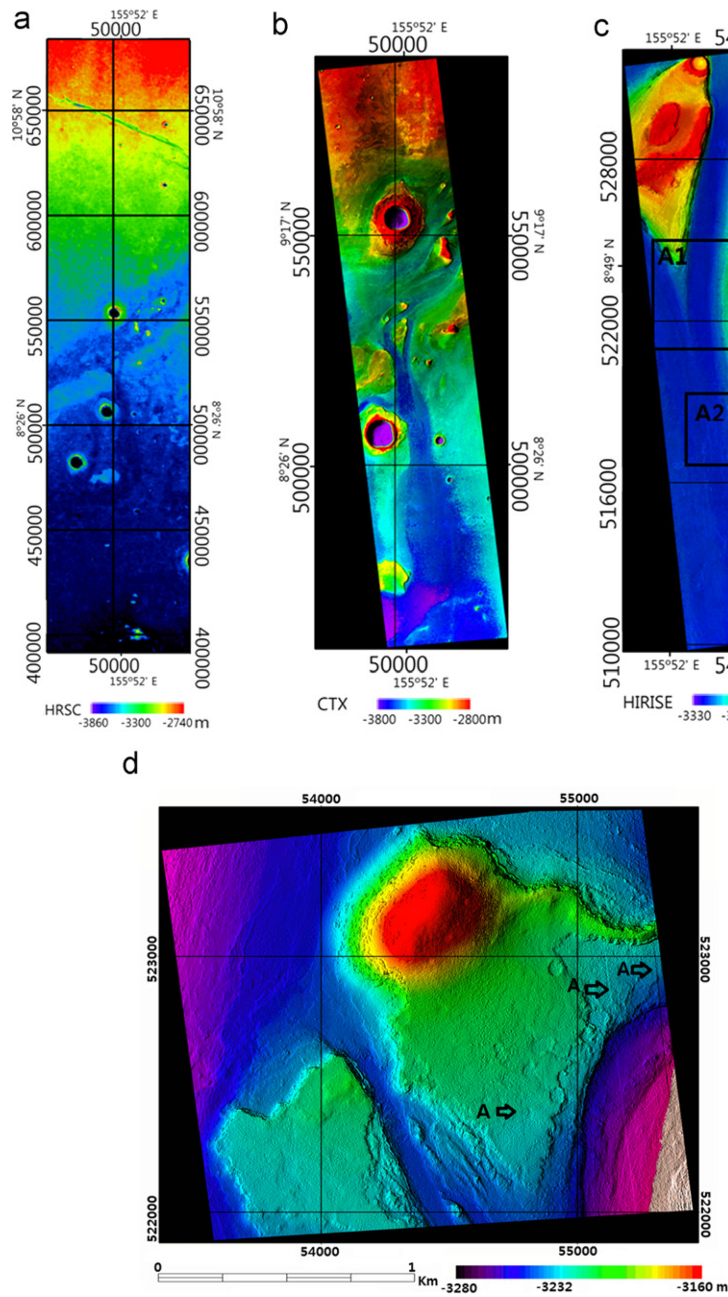

Fig. 3. The CTX and HiRISE topographic products in Athabasca Valles. (a) 50 m HRSC DTM over Athabasca Valles by DLR-VICAR photogrammetric S/W and our stereo matching system. (b) 18 m resolution CTX DTM over central channel. (c) 2.5 m HiRISE DTM in teardrop island. See Fig. 9(d) and (e) for the detailed VR implementations over A1 and A2 subareas. (d) 0.75 m refined DTM in sub area of Athabasca (middle east part of (c)). Note the artifact in left part by jitter effect.

generated and compared with MOLA height points for determination of accuracy. By oversampling of HRSC and CTX and downsampling of HiRISE stereo height points to an identical 18 m resolution, the artifact issue can be partly addressed. Then through profiles crossing MOLA tracks and the comparison data sets, the differences between the individual stereo and MOLA height can be determined. The profiles illustrating in Eberswalde crater and Athabasca Valles are shown, respectively, in Figs. 4 and 5.

The comparison results between MOLA height points and CTX stereo DTMs demonstrated extremely good agreement except a few rough topographies such as the apex of crater rim and the crater bottom (labels B1–B3 in Fig. 4(b) and (c)). The relatively large height discrepancies between MOLA and CTX DTMs in such steep areas likely resulted from the ill behaved image matching effects in the highly illuminated area of crater rim or the fully shadowed crater bottom. On the other hand, the size difference between MOLA footprint (about 150 m) and CTX stereo grid (<20 m) can be proposed as another reason for the height discrepancy.

From the statistics, it was realized that mostly the height difference between MOLA and CTX stereo DTM is within 10–30 m, as listed in Table 1 and Figs. 4 and 5. Especially it should be noted that the stereo height in the hydrological channels and the deposits showed constantly low discrepancies compared with MOLA within 10 m ranges (see labels C1–C5 in the track profiles illustrated in Figs. 4 and 5).

The HiRISE DTM also showed good agreements with MOLA except for small discrepancies over part of highly sloped area (Figs. 4(d), (e) and 5(d)). The source of this height difference was probably the

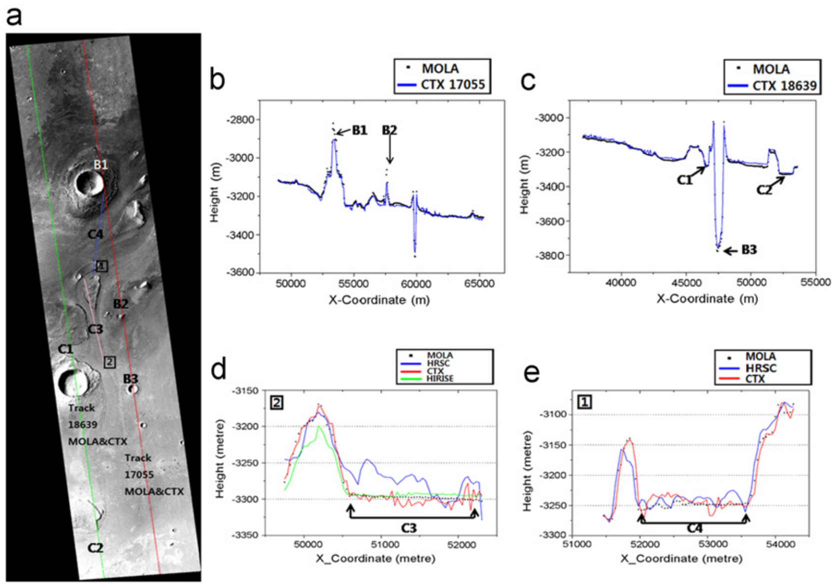

Fig. 4. The MOLA track profile crossing Athabasca data sets. (a) The location of track profiles. (b) CTX comparison profile in MOLA track number 17055. (c) CTX comparison profile in MOLA track number 18639. (d) MOLA comparison with HiRISE, CTX,HRSC in location 2. (e) MOLA comparison with HiRISE, CTX,HRSC in location 1.

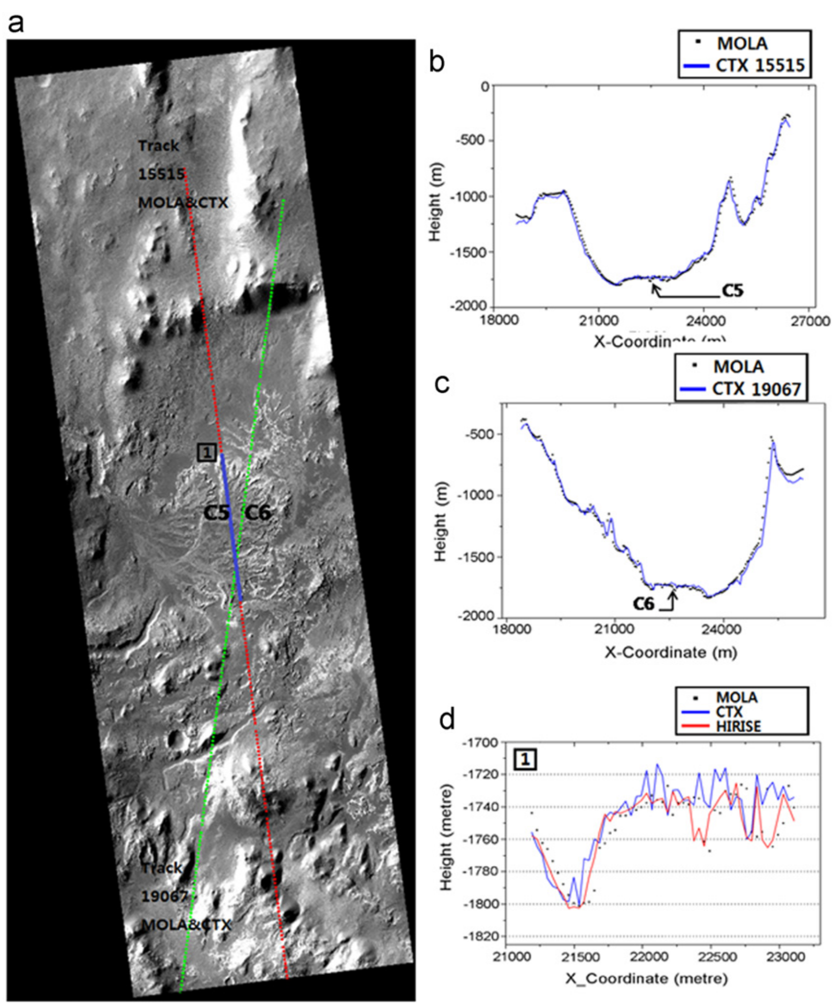

Fig. 5. The MOLA track profile crossing Eberswalde data sets. (a) The location of track profiles. (b) CTX comparison profile in MOLA track number 15515. (c) CTX comparison profile in MOLA track number 190667. (d) MOLA comparison with HiRISE, CTX,HRSC in location 1.

height re-sampling effect from 1–18 m for the height comparison and the MOLA laser beam interaction with local height variation (see the detail discussion of such effects in Kim and Muller, 2008).

Additionally, in more intrinsic aspects, the reasons of height discrepancy between stereo DTMs were summarized as: (1) the different sensor modeling originated the tracking accuracy of different spacecrafts, which composed the initial sensor model, and (2) incomplete geodetic control still exists especially in CTX and HiRISE because of the significant resolution different between CTX and HiRISE images. Refer to Kim and Muller (2009) about the detailed description of these height differences and the influences on topographic analysis.

The final issue in stereo DTM quality assessment is the geodetic accuracy of mosaic products. In this study, two mosaic products, i.e. mosaic DTM by two CTX stereo analyses and two HiRISE DTMs superimposed over CTX DTMs, were produced. There are no bundle block adjusted products but if individual stereo analysis is correctly controlled, it should not include any significant offsets between DTMs. Fig. 6(a) shows two profiles crossing HiRISE–CTX–HiRISE mosaicked products of Fig. 2(c). The profiles include a little offsets less than few meters between CTX–HIRISE and HiRISE–CTX boundaries. It is proof that CTX and HiRISE products which were individually extracted co-aligned in the identical absolute coordinate. The MOLA track profiles passing CTX and HiRISE DTMs in Fig. 6(b) is another strong evidence of the high geodetic quality of stereo products because the discrepancies over CTX and HiRISE DTMs demonstrate a few meter scale errors.

Conclusively, the overall stereo products employed for VR implementation can provide a seamless and geodetically verified exploration environment. It is the most distinguished merit of this implementation.

Table 1
Evaluation values of topographic products compared with MOLA.

HRSC-MOLA (m)	CTX-MOLA (m)	HIRISE-MOLA (m)
Athabasca Valles		
Mean: −4.879	Mean: −4.179	Mean: 9.721
Max: 219.100	Max: 97.808	Max: 45.384
Min: −415.750	Min: −89.580	Min: −9.366
Stddev: 23.487	Stddev: 13.696	Stddev: 15.227
Eberswalde crater		
Mean: −1.835	Mean: 9.973	Mean: 2.383
Max: 212.560	Max: 84.003	Max: 65.371
Min: −137.860	Min: −54.638	Min: −42.10
Stddev: 32.011	Stddev: 28.267	Stddev: 13.529

3. Virtual reality implementation

Since the co-registration of multi-resolution DTMs was precisely achieved, an effective 3D visualization of the co-registered DTMs is another important task. As the DTMs had already been co-aligned on an identical reference system, they now could be integrated altogether in a correct geodetic position. By adjusting the data format and transparency, different sources of DTMs could be readily applied to the hardware and software facilities described below.

3.1. Hardware components

A typical simulation process requires volume data visualization. Considering the usage of multiple high-resolution topographic products, the visualization system developed in this study aimed to employ supercomputing facility for manipulating terabyte (TB) scale data. Moreover, a large-scale visualization environment was proposed for efficient human–computer interaction. To this end, cluster computer architecture was firstly organized, in which a total

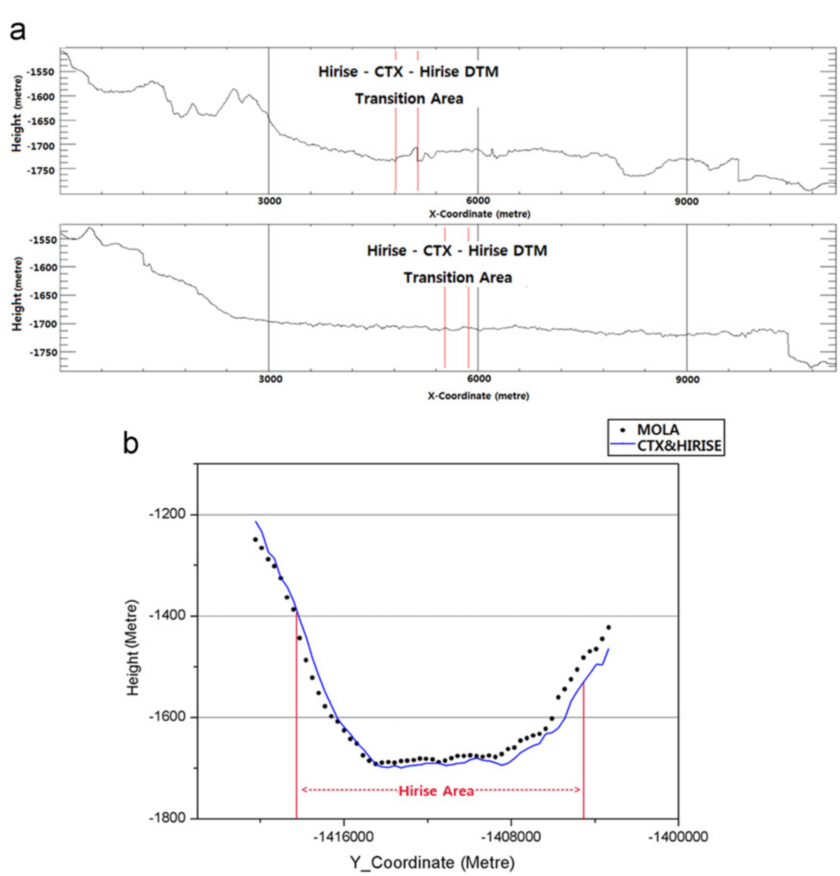

Fig. 6. The assessments of combined topographic products. (a) The height profiles in CTX and two HiRISE overlays (see Fig. 2 to identify the profile locations). (b) The height profiles in CTX and two HiRISE overlays with MOLA (see Fig. 2 to identify the profile locations).

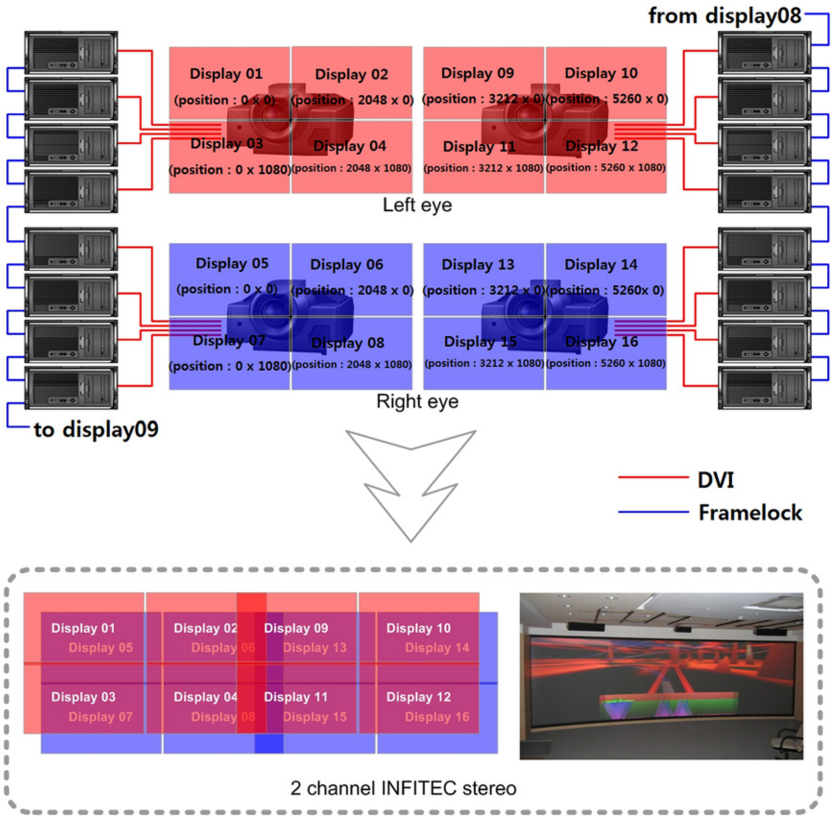

Fig. 7. Stereo view composition of the KISTI visualization system.

of 90 InfiniBand connected rendering nodes QuadroFX5600 GPU equipment with balanced 45TB file I/O are the main components. For interactive virtual reality presentation, real-time rendering was achieved by applying a high definition screen and 16 nodes of 4 core 2 socket Intel Xeon 5450 3.0 GHz system with NVIDIA QuadroFX5600 GPU. As shown in Fig. 7, the left and right eye stereo view is constructed using two sets of 8 rendering nodes. For a large scale presentation, four of the SONY projectors with 4096×2160 resolution were arranged to reach 18% overlapping. The projected images were then blended with a 7308 pixels $\times$ 2116 pixels resolution environment, so that they could be shown on a 2 m $\times$ 7.2 m interactive VR presentation screen.

3.2. Topographic data conversion

VR navigation has been implemented using DeltaGen software developed by RealTimeTechnology (RTT, 2010) AG. The software extensively adopted the cluster computer's GPU computing power to provide real-time global illumination. RTT suites and the visualization system produced a unique visualization environment for typical CAD/CAS based industrial requirements.

To close the gap between interactive CAD data processing and GeoTiff based topographical image processing, the GeoTiff data were converted for VR navigation using commercial software. With the software, the topographical data were converted to StereoLithography (STL, Ennex, 1999). The texture mapping was then performed using RTT DeltaGen again.

4. Results and discussion

The phenomenon of manipulation of Martian stereo products using facilities provided by KISTI is recorded in Fig. 8. Due to the powerful parallel processor, the 3D maneuvering of VR surface was performed without time lag in the test scene. Judging from the performance of the interactive control, it was found that the constructed VR provided great potential not only to replace the field trip but also to simulate the rover movements in the compressed time domain. The base topographies created in this paper for VR scene are shown in Fig. 9. It is observed that the detailed landscapes are sufficient for the interpretation of Martian geomorphology. The interesting features, such as hill side (Fig. 9(a) and (b)), meter scale terrace (Fig. 9(c)), fractures (Fig. 9(d)) and small mound (see Fig. 9(e)), are well presented.

However, the zooming up view from the ground surface as the close height of stereo camera equipped on the rover revealed that the performance of noise reduction and the current resolution of 3D topography were not fully addressed yet for some applications. As shown in Fig. 9(e), the detailed structures of cone shapes are not fully described by virtual reality constructed from a 2–3 m observer height. It means that stereo point cloud with higher density (<1 point/1 m) is required for some simulated situations. For example, the improved stereo height points are necessary for the visual inspection of risk elements for rover navigation or the interpretation of some detailed features for geomorphic research from a sub-meter vertical height.

The other technical issue occurring in the constructed VR scheme was the limitation of compatible format for rendering comprehensive topographic data set. In general, the commercial VR software manipulates the data set as the industrial vector format. The format issue limits the manipulation of few square km spatial data with 1.5 m grid spacing DTM and 40 cm resolution ortho-image (e.g. HiRISE stereo products). Thus, virtual realities established in this research were only in sub-set part of extracted data from the pre-processor.

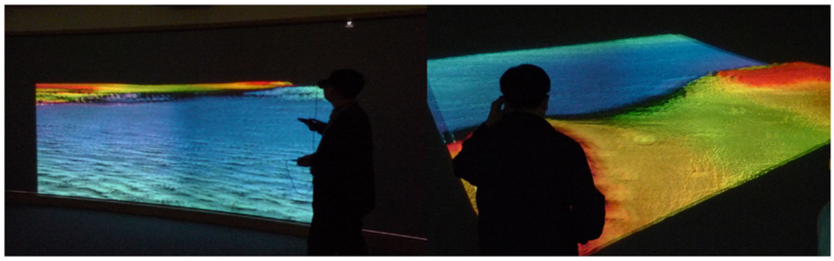

Fig. 8. Virtual Reality with Martian stereo products and facilities provided by KISTI.

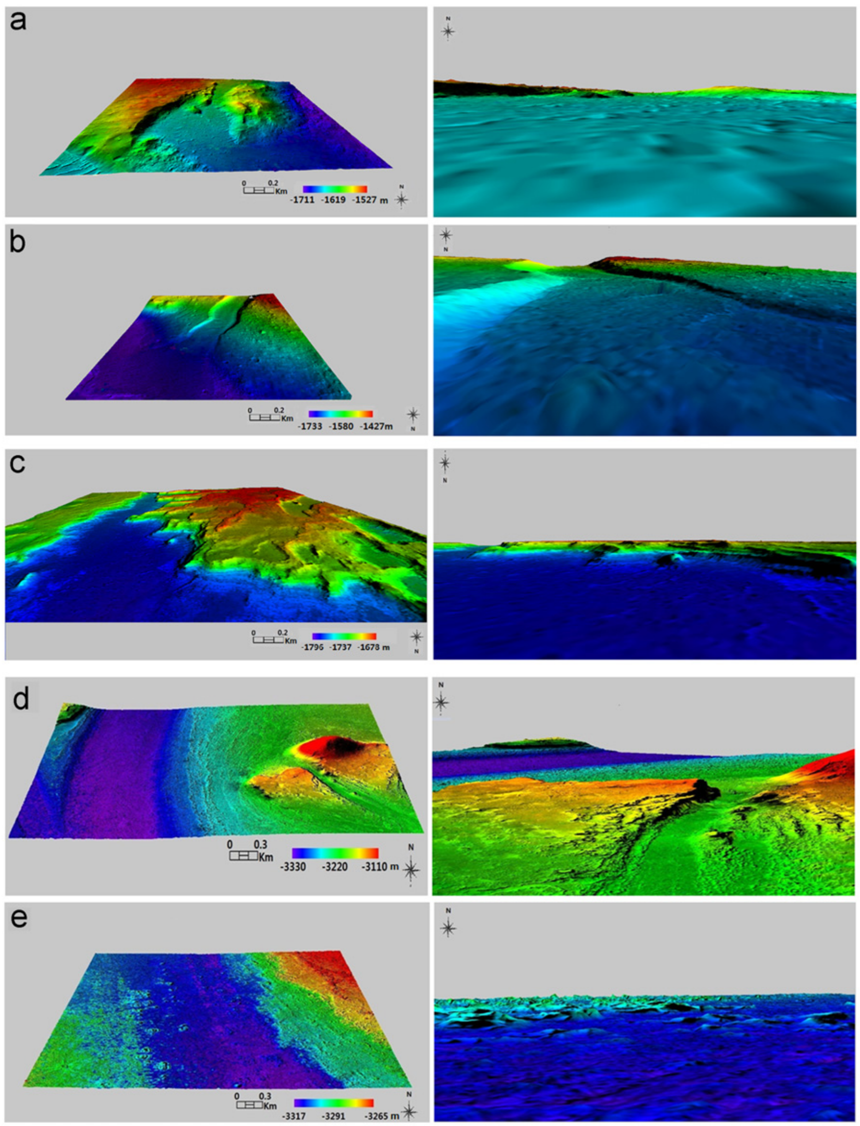

Fig. 9. Detailed topographies of Martian VR. (a) Eberswalde region 1. (b) Eberswalde region 2. (c) Eberswalde region 3. (d) Athabasca region 1. (e) Athabasca region 2.

5. Conclusions

The work performed in this study demonstrates how contemporary modern photogrammetry and scientific visual technology could be employed to reconstruct a virtual Martian surface. The VR implementation was highlighted by geodetically controlled topographic products covering medium to very high-resolution topographic products. The capability is unique and highly valuable for quantity analyses in scientific researches. Moreover, the high speed parallel processors connected to multiple beam projectors and 3D pointing devices produced unique features for almost real-time movement with a huge topographic input material in the VR environment. In order to accomplish landing site section and the rover transversing in the developed VR scheme, the close range photogrammetric technique will be integrated with the high speed simulator.

However, two problems remained unsolved in our VR implementation scheme. Firstly, the VR software does not support full sets of topographic data processed in our stereo processing line. Therefore employing an indigenous virtual environment based on industrial standard such as Synthetic Environment Data Representation and Interchange Specification (SEDRIS, 2010) has been proposed. The merit of the SEDRIS is that all environmental elements, including atmospheric factors, topographic blunders and any other risk elements, will be able to synthetically interact with the constructed topography. Secondly, improvement of spatial resolution of the 3D products is required for some applications. Since the density of stereo height points has reached the technical limit, other possible solutions, e.g. multiple image shape from shading technique (Lohse et al., 2006), will be further examined.

Conclusively, the quality of the topographic products created in this paper has been verified adopting the quantitative analysis and the visual evaluation conducted during VR implementation. The integration of created topographic products and the processing facilities has demonstrated the feasibility although a number of technical barriers for practical applications exist. To address the issues, an upgrade based on the VR scheme will be carried out to achieve an ultrafine Martian environment simulation. Also, the overall parallelized and high accuracy topographic processor will be continuously promoted for various possible applications.

Acknowledgments

The authors would like to acknowledge the KISTI for providing all H/Ws and S/Ws for Virtual reality experiment. Special thanks were given to Prof. Sanjeev Gupta and Dr. Nicolas Werner at Imperial College London for their kind discussion about geomorphology of the testing area. The authors acknowledge Prof. G. Neukum, PI of HRSC instrument for providing HRSC data and DLR VICAR S/W applied in this paper. The second author would like to thank the support from the National Science Council, Taiwan (project number: NSC 99-2218-E-004-001).

References

Albertz, J., Attwenger, M., Barrett, J., Casley, S., Dorninger, P., Dorrer, E., Ebner, H., Gehrke, S., Giese, B., Gwinner, K., Heipke, C., Howington-Kraus, E., Kirk, R.L., Lehmann, H., Mayer, H., Muller, J.P., Oberst, J., Ostrovskiy, A., Renter, J., Reznik, S., Chmidt, R., Scholten, F., Spiegel, M., Stilla, U., Wahlisch, M., Neukum, G., 2005. HRSC CoI-Team, 2005. HRSC on Mars express—photogrammetric and cartographic research. Photogrammetric Engineering and Remote Sensing 71 (10), 1153–1166.

Anderson, J.A., Sides, S.C., Soltesz, D.L., Sucharski, T.L., Becker, K.J., 2004. Modernization of the integrated software for imagers and spectrometers. In: Proceedings of the 35th Lunar and Planetary Science Conference, abstract #2039. Houston, USA (on CD-ROM).

Burr, D.M., Grier, J.A., McEwen, A.S., Keszthelyi, L.P., 2002. Repeated aqueous flooding from the Cerberus Fossae: evidence for very recently extant, deep groundwater on Mars. Icarus 159 (1), 53–73.

Day, T., Muller, J.-P., 1989. Digital elevation model production by stereo-matching SPOT image-pairs: a comparison of algorithms. Image and Vision Computing 7 (2), 95–101.

Dowman, I., Dolloff, J.T., 2000. An evaluation of rational functions for photogrammetric restitution. International Archive of Photogrammetry and Remote Sensing 33 (Part B3), 254–266.

Ennex, 1999. STL (Standard Data Format) ⟨http://www.ennex.com/~fabbers/StL.asp⟩, [Accessed September 28, 2010].

Fraser, C.S., Dial, G., Grodecki, J., 2006. Sensor orientation via RPCs. ISPRS Journal of Photogrammetry and Remote Sensing 60 (3), 182–194.

Gardner, C.S., 1992. Ranging performance of satellite laser altimeters. IEEE Transaction on Geoscience and Remote Sensing 30 (5), 1061–1072.

Gruen, A., 1985. Adaptive least squares correlation: a powerful image matching technique. South Africa Journal of Photogrammetry, Remote Sensing and Cartography 14 (3), 175–187.

Gwinner, K., Scholten, F., Jaumann, R., Roatsch, T., Oberst, J., Neukum, G., 2007. Global mapping of Mars by systematic derivation of Mars Express HRSC high-resolution digital elevation models and orthoimages. In: Proceedings of the ISPRS Working Group IV/7 Workshop. Houston, USA (on CD-ROM).

Head, J.H., Wilson, L., Mitchell, K.L., 2003. Generation of recent massive water floods at Cerberus Fossae, Mars by dike emplacement, cryospheric cracking, and confined aquifer groundwater release. Geophysical Research Letters 30 (11), 1577. doi:10.1029/2003GL017135.

Heipke, C., Oberst, J., Albertz, J., Attwenger, M., Dorninger, P., Dorrer, E., Ewe, M., Gehrke, S., Gwinner, K., Hirschmuller, H., Kim, J.R., Kirk, R.L., Mayer, H., Muller, J.-P., Rengarajan, R., Rentsch, M., Schmidt, R., Scholten, F., Shan, J., Spiegel, M., Wählisch, M., Neukum, G., HRSC Co-Investigator Team, 2007. Evaluating planetary digital terrain models—the HRSC DTM test. Planetary and Space Science 55, 2173–2191.

Jaeger, W., Keszthelyi, L.P., McEwen, A.S., Dundas, C.M., Russell, P.S., 2007. Athabasca Valles, Mars: a lava-draped channel system. Science 317, 1709–1711.

Jaeger, W., Keszthelyi, L.P., Skinner, J.A., Mailazzo, M.P., McEwen, A.S., Titus, T.N., Rosiek, M.R., Gulaszka, D.M., Howington-Kraus, E., Kirk, R.L., 2010. HiRISE Team, 2010. Emplacement of the youngest flood lava on Mars: a short, turbulent story. Icarus 205 (1), 230–243.

Jaumann, R., Neukum, G., Behnke, T., Duxbury, T.C., Eichentopf, K., Flohrer, J., Gasselt, S.V., Giese, B., Gwinner, K., Hauber, E., Hoffmann, H., Hoffmeister, A., Kohler, U., Matz, K.-D., McCord, T.B., Mertens, V., Oberst, J., Pischel, R., Reiss, D., Ress, E., Roatsch, T., Saiger, P., Scholten, F., Schwarz, G., Stephan, K., Wahlisch, M., 2007. the HRSC Co-Investigator Team, 2007. The high-resolution stereo camera (HRSC) experiment on MarsExpress: instrument aspects and experiment conduct frominterplanetary cruise through the nominal mission. Planetary and Space Science 55 (2007), 928–952.

Jerolmack, D.J., Mohrig, D., Zuber, M.T., Byrne, S., 2004. A minimum time for the formation of Holden Northeast fan, Mars. Geophysical Research Letter 31, L21701. doi:10.1029/2004GL021326.

Kim, J.R., Muller, J.P., 2008. Very high resolution stereo DTM extraction and its application to surface roughness estimation over Martian surface. International Archives of the Photogrammetry, Remote Sensing and Spatial Information Sciences 37 (B4), 993–998.

Kim, J.R., Muller, J.-P., Balme, M., Murray, J.B., 2007. Geometric ground control of very high resolution imagery using HRSC intersection points and a non-rigorous camera model. In: Proceedings of the 38th Lunar and Planetary Science Conference, abstract #1338. Houston, USA: 1811-1812 (on CD-ROM).

Kim, J.R., Muller, J.P., 2009. Multi-resolution topographic data extraction from Martian stereo imagery. Planetary and Space Science 57 (15), 2095–2112.

Kirk, R.L., Howington-Kraus, E., Redding, B.R., Galuszka, D., Hare, T.M., Archinal, B.A., Soderblom, L.A., Barrett, J.M., 2003. High resolution topomapping of candidate MER landing sites with Mars Orbiter Camera narrow-angle images. Journal of Geophysical Research 108 (E12), 8088. doi:10.1029/2003JE002131.

Kirk, R.L., Howington-Kraus, E., Rosiek, M.R., Anderson, J.A., Archinal, B.A., Becker, K.J., Cook, D.A., Galuszka, D.M., Geissler, P.E., Hare, T.M., Holmberg, I.M., Keszthelyi, L.P., Redding, B.L., Delamere, W.A., Gallagher, D., Chapel, J.D., Eliason, E.M., King, R., McEwen, A.S., 2008. HiRISE Team, 2008. Ultrahigh resolution topographic mapping of Mars with MRO HiRISE stereo Images: meter-scale slopes of candidate Phoenix landing sites. Journal of Geophysical Research 113 (E00A24). doi:10.1029/2007JE003000.

Lewis, K.W., Aharonson, O., 2006. Stratigraphic analysis of the distributary fan in Eberswalde crater using stereo imagery. Journal of Geophysical Research 111, E06001. doi:10.1029/2005JE002558.

Lin, S.Y., Muller, J.P., Mills, J.P., Miller, P.E., 2010. An assessment of surface matching for the automated co-registration of MOLA, HRSC and HiRISE DTMs. Earth and Planetary Science Letters 294 (3–4), 520–533.

Lohse, V., Hepike, C., Kirk, R.L., 2006. Derivation of planetary topography using multi-image shape-from-shading. Planetary and Space Science 54, 661–674.

Malin, M.C., Bell, J.F., Cantor, B.A., Caplinger, M.A., Calvin, W.M., Clancy, R.T., Edgett, K.S., Edwards, L., Haberle, R.M., James, P.B., Lee, S.W., Ravine, M.A., Thomas, P.C., Wolff, M.J., 2007. Context Camera investigation on board the Mars Reconnaissance Orbiter. Journal of Geophysical Research 112 (E05S04). doi:10.1029/2006JE002808.

Malin, M.C., Edgett, K.S., 2003. Evidence for persistent flow and aqueous sedimentation on early Mars. Science 302, 1931–1934. doi:10.1126/science.1090544.

McEwen, A.S., Eliason, E.M., Bergstrom, J.W., Bridges, N.T., Hansen, C.J., Delamere, W.A., Grant, J.A., Gulick, V.C., Herkenhoff, K.E., Keszthelyi, L., Kirk, R.L., Mellon, M.T., Squyres, S.W., Thomas, N., Weitz, C.M., 2007. Mars reconnaissance orbiter's high resolution imaging science experiment (HiRISE). Journal of Geophysical Research 112 (E05S02). doi:10.1029/2005JE002605.

McEwen, A.S., Preblich, B.S., Turtle, E.P., Artemieva, N.A., Golombek, M.P., Hurst, M., Kirk, R.L., Burr, D.M., Christensen, P.R., 2005. The rayed crater Zunil and interpretations of small impact craters on Mars. Icarus 176, 351–381.

Moore, J.M., Howard, A.D., Dietrich, W.E., Schenck, P.M., 2003. Martian layered fluvial deposits: implications for Noachian climate scenarios. Geophysical Research Letter 30 (24), 2292. doi:10.1029/2003GL019002.

Murray, J., Muller, J.P., Neukum, G., Werner, S.C., van Gasselt, S., Hauber, E., Markiewicz, W.J., Head, J.W., Foing, B.H., Page, D., Mitchell, K.L., Portyankina, G., 2005. HRSC Co-Investigator Team, 2005. Evidence from the Mars express high resolution stereo camera for a frozen sea close to Mars' equator. Nature 434, 352–356.

Neumann, G.A., Abshire, J.B., Aharonson, O., Garvin, J.B., Sun, X., Zuber, M.T., 2003. Mars orbiter laser altimeter pulse width measurement and footprint-scale roughness. Geophysical Reviews 30 (11), 1561. doi:10.1029/2003GL017048.

Neumann, G.A., Rowlands, D.D., Lemoine, F.G., Smith, D.E., Zuber, M.T., 2001. Crossover analysis of Mars orbiter laser altimeter data. Journal of Geophysical Research 106 (E10), 23753–23768. doi:10.1029/2000JE001381.

Plescia, J.B., 2003. Cerberus Fossae, Elysium, Mars: a source for lava and water. Icarus 164 (1), 79–95.
RTT, 2010. RTT Suite, 〈http://www.realtime-technology.com/flash/index_eng.php#/237〉, (Accessed September 28, 2010).
Scholten, F., Gwinner, K., Roatsch, T., Matz, K.D., Wählisch, M., Giese, B., Oberst, J., Jaumann, R., Neukum, G., 2005. Mars Express HRSC data processing—methods and operational aspects. Photogrammetric Engineering and Remote Sensing 71 (10), 1143–1152.
SEDRIS, 2010. SEDRIS Technology, 〈http://www.sedris.org/〉, (Accessed September 28, 2010).
Smith, D.E., Zuber, M.T., Frey, H.V., Garvin, J.B., Head, J.W., Muhleman, D.O., Pettengill, G.H., Phillips, R.J., Solomon, S.C., Zwally, H.J., Banerdt, W.B., Duxbury, T.C., Golombek, M.P., Lemoine, F.G., Neumann, G.A., Rowlands, D.D., Aharonson, O., Ford, P.G., Ivanov, A.B., McGovern, P.J., Abshire, J.B., Afzal, R.S., Sun, X., 2001. Mars Orbiter laser Altimeter: experiment summary after the first year of global mapping of Mars. Journal of Geophysical Research 106 (E10), 23689–23722.
Spiegel, M., 2007. Improvement of interior and exterior orientation of the three line camera HRSC with a simultaneous adjustment. International Archives of Photogrammetry and Remote sensing 36 (3/W49B), 161–166.
Tao, C.V., Hu, Y., 2002. 3D reconstruction methods based on the rational function model. Photogrammetric Engineering and Remote Sensing 68 (7), 705–714.
U.S. Geological Survey, 2009. Working with Mars Reconnaissance Orbiter HiRISE Data. 〈http://isis.astrogeology.usgs.gov/IsisWorkshop/index.php/Working_with_Mars_Reconnaissance_Orbiter_HiRISE_Data〉 (Accessed 25th April 2009).
Warner, N., Gupta, S., Kim, J.R., Lin, S.Y., Muller, J.P., 2010a. Hesperian equatorial thermokarst lakes in Ares Vallis as evidence for transient warm conditions on Mars. Geology 38 (1), 71–74.
Warner, N., Gupta, S., Lin, S.Y., Kim, J.R., Muller, J.P., 2010b. Late Noachian to Hesperian climate change on Mars: evidence of episodic warming from transient crater lakes near Ares Vallis. Journal of Geophysical Research, 115. doi:10.1029/2009JE003522.
Warner, N., Gupta, S., Muller, J.P., Kim, J.R., Lin, S.Y., 2009. A refined chronology of catastrophic outflow events in Ares Vallis, Mars. Earth and Planet Science Letter 288 (1), 58–69.
Zitnick, C.L., Kanade, T., 2000. A cooperative algorithm for stereo matching and occlusion detection. IEEE Transaction Pattern Analysis and Machine Intelligence 22 (7), 675–684.